Electrical Impedance of Piezoelectric Ceramics under Acoustic Loads

Francisco J. Arnold[*1], **Marcos S. Gonçalves**[*2],
Leonardo L. Bravo Roger[*3], and **Sérgio S. Mühlen**[**4], Non-members

ABSTRACT

The electrical impedance of piezoelectric ceramics is influenced by variations in its acoustic load. This is a very common situation for power ultrasonic applications in medicine where the irradiated media can present different interfaces and impedances to the propagating acoustic energy. In this work we analyzed the behavior of the resonances, anti-resonances and the effective electromechanical coupling factor of a piezoelectric ceramic ring vibrating in thickness mode. The analysis is based on equivalent electrical circuits and considers variations in the acoustic load. The results showed that the electrical impedance of the ceramic is altered with the characteristics of the acoustic load, resulting in new resonances and changing the effective electromechanical coupling factor. Electronic driving circuits for piezoelectric transducers must be able to dynamically adjust the frequencies when the acoustic load varies.

Keywords: Piezoelectric, Resonance, Acoustic Load, Electromechanical Coupling Factor, Thickness Mode.

1. INTRODUCTION

Most of ultrasonic systems use piezoelectric transducers as generators of acoustic energy. In these transducers the electrical energy supplied by electronic sources is converted into mechanical vibrations. Sinusoidal voltages are typically used to drive the transducers, at or close to its resonance. At resonance the transducer surface vibrates with maximum amplitude and the energy conversion becomes more efficient. Whenever the physical characteristics of the electro-acoustical system are altered, a more or less severe tuning and efficiency loss can occur.

Physical variations on the propagation media are very common in most ultrasonic applications. For instance, in therapeutic or diagnostic medical ultrasound, the mechanic vibrations travel across body structures whose acoustic impedances may vary considerably. These alterations in the propagation media result in variations in the impedance along the frequency spectrum and resonance frequencies shifting.

Tuning losses between piezoelectric transducer and electronic source may also be caused by the heating (and consequent dilatation) of the transducer parts due to internal friction, mainly on large vibration amplitude, caused by higher electrical excitation [1-3], by variations in the mechanical pre-stressing bias [4, 5], and variations in the characteristics of the radiated media [6].

The typical behavior of the electrical impedance of piezoelectric transducers in the resonance neighborhood is characterized by abrupt variations. Therefore small shifting of resonance corresponds to large variations in the electrical behavior of the transducer. In the whole system, these variations frequently cause mismatching between the transducer and the electronic driving circuit. By consequence, the performance of the system is affected, the vibration amplitude decreases, as well as the energy conversion rate and the acoustic energy on the radiated media.

These drawbacks are more evident in sandwiched piezoelectric transducers, and tuning corrections are needed. They are usually performed in the electronic circuitry by PLL (Phase-Locked Loop) oscillators [7-9] and harmonic cancellation techniques [10].

Piezoelectric ceramic transducers are often subjected to changes in its acoustic load. In medical applications, for instance, mainly in power applications when ultrasonic therapeutic tools are used, these changes occur when the transducer interacts with biological tissues or interfaces of different acoustic impedances [11].

The scientific literature abounds with studies on the effect of mechanical loads [6], backing [12], matching [12-14], losses [15-17] and bandwidth [17, 18] on the behavior of the electrical impedance of piezoelectric transducers. Shuyu [6] studied the effects of mechanical loads on the resonance of sandwiched piezoelectric transducers. He has found that the resonance dependence on the acoustic load, cross-section area and frequency may be described by a complex transcendental function. He also pointed out appropriately the high complexity of the mathematical analysis of this problem.

The present work aims to study the effects of the

Manuscript received on August 27, 2014 ; revised on November 26, 2014.

* The authors are with Department of Telecommunication Division, School of Techonology, University of Campinas, Brazil, Email: arnold@ft.unicamp.br[1], marcos@ft.unicamp.br[2] leobravo@ft.unicamp.br[3]

** The author is with Department of Biomedical Engineering, Faculty of Electrical and Computer Engineering, University of Campinas, Brazil, Email: smuhlen@ceb.unicamp.br[4]

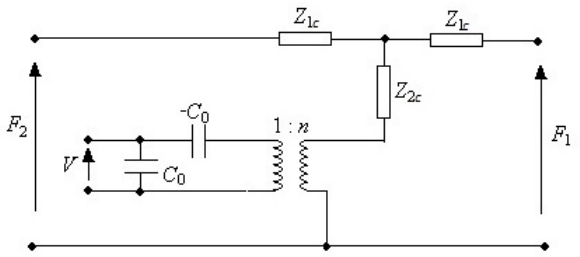

Fig.1: *Mason's equivalent circuit for a piezoelectric ceramic plate on thickness mode.*

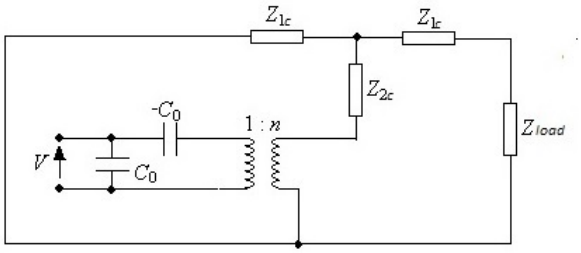

Fig.2: *Equivalent electrical circuit of the loaded transducer.*

acoustic load on the electrical impedance of a ceramic ring to get physical insights, from a simpler structure than that shown in [6]. This seemed to be a new and better approach to the subject.

We describe the electrical impedance behavior of a piezoelectric ceramic vibrating on thickness mode and subjected to increasing acoustic load. We have registered the resulting shift of resonance frequencies and the effective electromechanical coupling factor, as well as the appearance of new resonances peaks, at frequencies near the resonance of the unloaded piezoelectric ceramic. The limited frequency range has been chosen in order to discard any lateral or radial vibration modes in the vicinity of the working frequency.

The Mason's equivalent circuit [19-20] was used to represent the electrical behavior of the piezoelectric ring vibrating in the thickness mode at resonance. This ring was loaded by a column of water whose height was precisely adjusted. The frequency spectrum of the piezoelectric transducer was measured with different heights of the water column. Resonances, anti-resonances and the effective electromechanical coupling factor were analyzed. The results may be considered for designing of electronic circuits to correct resonances of piezoelectric transducers.

2. ELECTROMECHANICAL EQUIVALENT CIRCUIT

Among several methods to analyze piezoelectric transducers, the equivalent electromechanical circuit is one of the most popular. We considered a piezoelectric ring with thickness l and flat surfaces of area A. When in loss-free condition, the ceramic has physical properties defined as $v, \rho, c_{33}^D, \varepsilon_{33}^S$ and $h33$ being respectively the propagation wave velocity, density, and elastic (with electrical displacement null), dielectric (with strain null) and piezoelectric coefficients. The characteristic impedance is $Z_c = \rho \cdot v \cdot A$.

The literature shows many equivalent circuits for piezoelectric devices [19-22]. Mason's 1-D model is proposed here to study the electrical impedance of the piezo-transducer excited on thickness mode. Figure 1 shows Mason's model electrical circuit.

The components of the circuit shown in Figure 1 are described by Equations 1-3:

$$Z_{1c} = \mathrm{j} Z_c \tan(kl/2) \tag{1}$$

$$Z_{2c} = -\mathrm{j} Z_c \csc(kl) \tag{2}$$

$$n = h_{33} C_0 \tag{3}$$

where
$k = \omega/v$ [m^{-1}];
ω is the angular frequency [rad/s];
j is the complex number $\sqrt{-1}$;
h_{33} is the piezoelectric coefficient [N/C];
C_0 is the intrinsic capacitance of the piezoelectric ceramic, given by:

$$C_0 = \varepsilon_{33}^S \frac{A}{l} \tag{4}$$

In addition, V is the voltage applied to the transducer electrodes; i is the current through the transducer; F_1 and F_2 are the forces on the flat surfaces of the ceramic.

Port 1 of the transducer has been loaded. The acoustic load is represented by a T-network [23] with short-circuited output. The load (water) is physically characterized by v_a, ρ_a and Z_a, respectively velocity of wave propagation, density and characteristic impedance. Equation 5 gives the acoustic impedance of the load:

$$Z_{load} = Z_a tan(k_a l_a) \tag{5}$$

where
$Z_a = \rho_a \cdot v_a \cdot A$ is the characteristic acoustic impedance of the load [kg/s].
$k = \omega/v_a$ [m^{-1}];
v_a is the propagation wave velocity in the acoustic load [m/s];
l_a is the height of liquid column [m].

Port 2 is short-circuited because it is free to vibrate on air. The equivalent circuit of the whole system is shown in Figure 2:

The electrical impedance "seen" from the electrical port of the transducer is:

$$Z = X_{C0} + Z_{m1} + Z_{m2} \tag{6}$$

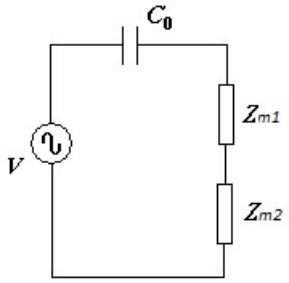

Fig.3: *Serial association of impedances of the loaded transducer equivalent electrical circuit.*

where

K is the static electromechanical coupling factor

$$K^2 = \frac{h_{33}^2 \varepsilon_{33}^S}{c_{33}^D} \tag{7}$$

$$Z_{m1} = X_{C0}\left[K^2 \frac{\tan(kl)}{kl/2} \frac{Z_c \tan(kl/2)}{Z_c \tan(kl) + Z_a \tan(k_a l_a)}\right] \tag{8}$$

$$Z_{m2} = X_{C0}\left[K^2 \frac{\tan(kl)}{kl/2} \frac{(Z_a/2) \tan(k_a l_a)}{Z_c \tan(kl) + Z_a \tan(k_a l_a)}\right] \tag{9}$$

$$X_{c0} = \frac{-j}{\omega C_0} \tag{10}$$

A serial electrical circuit of C_0, Z_{m1} and Z_{m2} is shown in Figure 3.

The effective electromechanical coupling factor keff [24, 25] is determined by:

$$k_{eff}^2 = 1 - \left(\frac{f_r}{f_a}\right)^2 \tag{11}$$

where

f_r is the resonance frequency [Hz];

f_a is the anti-resonance frequency [Hz].

The electromechanical coupling factor is a dimensionless value used to express the rate of energy conversion in the piezoelectric process [24]. The static electromechanical coupling factor is used in restricted investigations on particular shapes of crystals excited by low levels of electrical and mechanical fields. In practice, the effective electromechanical coupling factor is adopted because it takes into account the material properties and geometrical shapes of the transducers [25].

3. MATERIALS AND METHODS

The ring-shaped piezoelectric ceramic (Thornton Inpec - SP, Brazil) used in the experiments have silver electrodes coated on both flat surfaces. This piezoelectric ceramic has been chosen among other samples because its resonance frequency for the thickness vibration mode is far from those of other modes. This particularity allowed us to observe the resonance deviations of the thickness mode only. The presence of other modes close to the investigated resonance

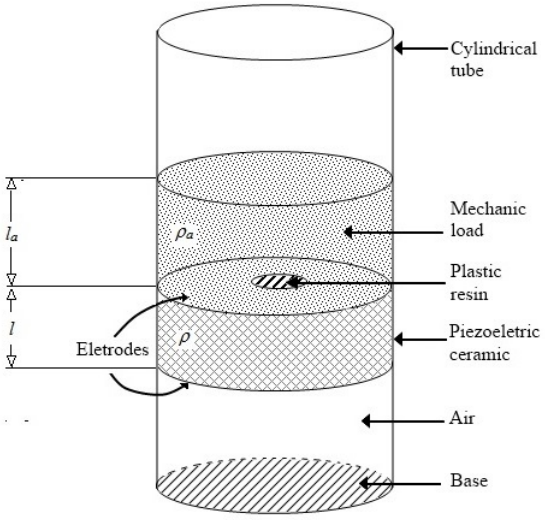

Fig.4: *Setup used for investigating the effects of the mechanical load on the piezoelectric transducer electrical impedance.*

makes difficult the observation of the effects of resonance shifting.

The physical properties of the piezoelectric ceramic are: v = 4450 m/s; ρ = 7600 kg/m^3; inner radius 6.3 mm; outer radius 19.0 mm; l = 6.3 mm; c_{33}^D =10.05×10^{10} N/m^2; ε_{33}^S = 11.0×10^{-9} F/m; h_{33} = 14.8×108 N/C.

The acoustic load is a column of water poured inside a plastic cylinder of thin wall. The diameter is the same of the ceramic ring, that is glued on the inside wall, blocking the bottom and avoiding water to leak. The cylinder is made of lightweight material, thus its mass is negligible and not considered in the modeling represented by Equation 6. A thin layer of plastic resin coats the electrode in the ceramic that is in contact with liquid. Figure 4 shows the schematic of this setup.

The frequencies spectra of the transducer were obtained using a HP4294A vector impedometer, and the resonances and anti-resonances determined considering the minimum and maximum values of the impedance modulus, respectively.

The propagation wave velocity v_a and the density of water ρ_a are, respectively, 1500 m/s and 1000 kg/m^3. The water was poured inside the tube in drops of 1 ml by means of a pipette. Each 1 ml poured corresponds to a 0.9 mm increase on the water column height. The measurements have been performed only after a minimum height of 2.7 mm because with smaller amounts there was not a uniform distribution of water on the ceramic surface, due to superficial tension of the liquid. The maximum height of the column was 16 mm.

The piezoelectric ring mechanically unloaded has resonance and anti-resonance around 328 and 353 kHz, respectively. The impedance behavior was ob-

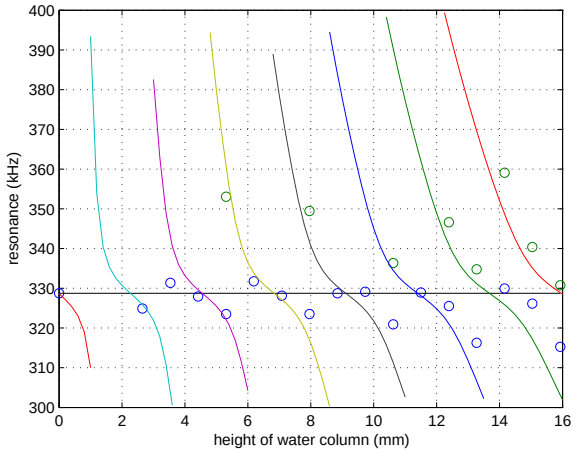

Fig.5: *Resonance as function of height of water column. Experimental data are marked as ∘. Calculated results are represented by continuous lines. The horizontal line is the resonance reference (328.743 kHz).*

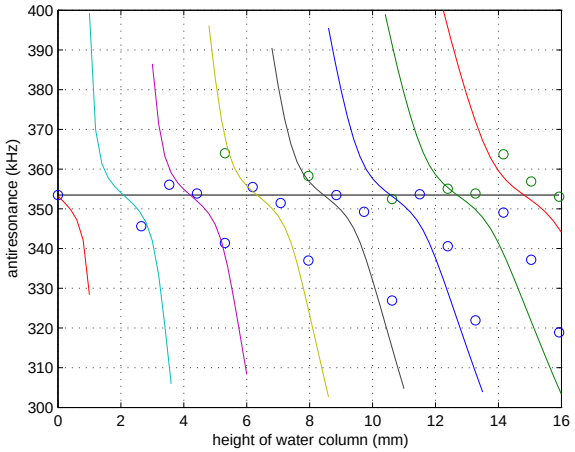

Fig.6: *Anti-resonance as function of height of water column. Experimental data are marked as ∘. Calculated results are represented by continuous line. The horizontal line is the anti-resonance reference (353.466 kHz).*

served in the range between 300 and 370 kHz. For each height of water column the resonances and anti-resonances were measured in the correspondent spectrum.

4. RESULTS AND DISCUSSION

The frequency spectrum of the unloaded piezoelectric ring was obtained first. The resonance and anti-resonance frequencies found were considered as reference values. They were: 328.743 kHz for resonance and 353.466 kHz for anti-resonance. The reference for k_{eff} is 0.37. At frequencies for which the denominator of Equation 6 is null, Z is maximum and the transducer works at anti-resonance. If there is no acoustical load, the denominator is $Z_c tan(kl)$. Adding load, new resonances appear in the spectrum due to term $Z_a tan(k_a l_a)$. As la increases, the curve corresponding to $Z_a tan(k_a l_a)$ moves downwards in the spectrum to smaller frequencies while the curve of $Z_c tan(kl)$ remains static. Combined effects of $Z_c tan(kl)$ and $Z_a tan(k_a l_a)$ yield new resonances.

Figures 5 and 6 show the resonance and anti-resonances as function of the water column height. The experimental data values are marked as small circles. Calculated values of Equation 6 are presented as continuous lines in the graphic.

The experimental results show that two resonances (or anti-resonances) have been found inside of the investigated frequencies span for some column heights. Repeated resonances for the same column height are distinguished in the graphic. Each calculated curve is well fitted to a set of experimental points, showing that successively resonances are displaced for smaller values when the height of the water column increases.

Anti-resonances are the roots of the denominator on the motional impedances of Equation 6. They can be found solving the equation with a numerical method. When the denominator is null, the components Z_{m1} and Z_{m2} present discontinuities, typical of the intrinsic behavior of tangent functions, therefore the magnitude of Z tends to infinity. Out of discontinuities, the motional impedance is dominated by Z_{m1}, once the characteristic mechanical impedance of the piezoelectric element is higher than that of load. The resonances are determined when the sum of impedances of the circuit components on Figure 3 is null. As well as in [6], we have also a transcendental equation (Equation 6) that defines the impedance, which does not allow us to find a closed-form for solution.

The separation between resonance and anti-resonance is related to the effective electromechanical coupling factor [20, 24, 25], such as observed in Equation 11. This separation can be evaluated studying the interaction of nulling Z and the discontinuities of motional impedances. First considering the transducer unloaded ($Z_{m2} = 0$), thus it will be the resonance when the electrical energy stored in the intrinsic capacitance is equal to kinetic energy in the ceramic mass. Z_{m1} signal is positive, denoting an inductive characteristic of the transducer impedance.

When the transducer is loaded, anti-resonances are modified due to influence of Z_{m2}, although Z_{m1} remains exhibiting preponderance on motional impedance. Anyway, the anti-resonance decreases if l_a increases. It should be noticed that anti-resonances depend only on the mechanical characteristics of the transducer elements.

At resonance there are three cases to be analyzed, which are evident in the spectrum shown in Figure 7. There, the calculated frequency spectrum contain

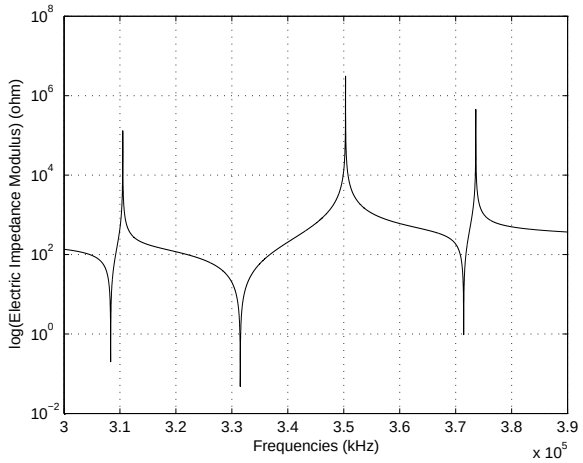

Fig.7: *Electrical impedance modulus as function of frequencies on the transducer with l_a = 13.2 mm.*

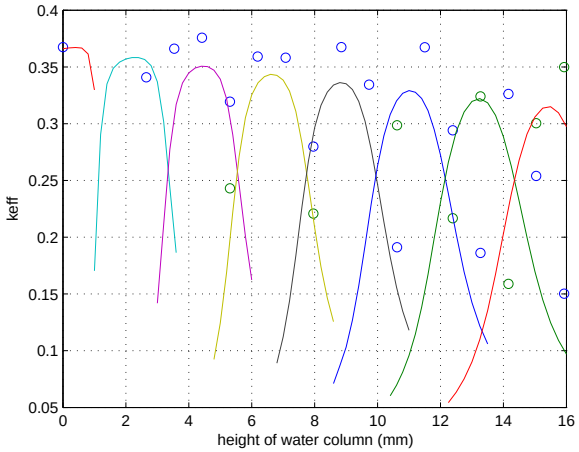

Fig.9: *Effective electromechanical coupling factor as function of height of water column. Experimental data are marked as ∘. Calculated results are represented by continuous lines. Horizontal line is k_{eff} reference (0.37).*

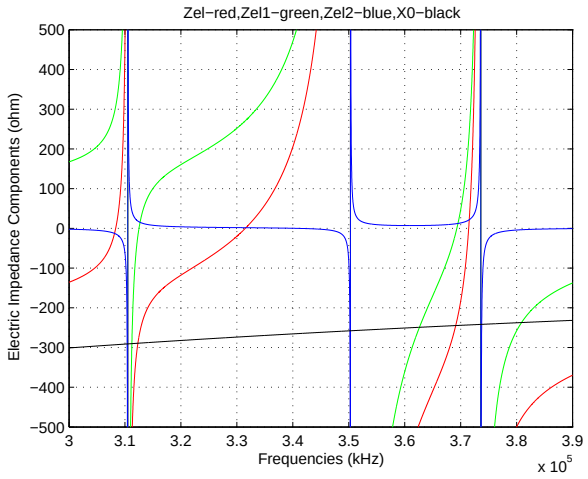

Fig.8: *Zoom of the complex representation of Z (red line), X_{C0} (black line), Z_{m1} (green line) and Z_{m2} (blue line) as function of frequencies.*

three pairs of resonance/anti-resonance frequencies related to l_a = 13.2 mm. Figure 8 shows the zoom of complex representation, where lines red, black, green and blue plot Z, X_{C0}, Z_{m1} and Z_{m2}, respectively. Resonances are found at frequencies which red line crosses the horizontal axis ($Z = 0$). In Figure 8, at central resonance, Z results basically of X_{C0} and Z_{m1}. In this case, as $Z_{oa}tan(k_a l_a)$ is often small, resonance (331.64 kHz) and anti-resonance (350.32 kHz) frequencies are closed to the reference values. This pair belongs to the curve 7 on Figures 5 and 6. Thus, the electromechanical coupling factor in this case (0.32) is close to the reference. A significant separation between resonance and anti-resonance in this vibration mode can be seen in Figure 7.

In the first (f_r = 308.04 kHz, f_a = 310.50 kHz, k_{eff} = 0.12) and in the third pair (f_r = 371.52 kHz, f_a = 373.50 kHz, k_{eff} = 0.10), Z is null at frequencies where Z_{m2} is not negligible and near a discontinuity. The difference among first and third pairs is the opposite signal of Z_{m2}. In both cases, the separation between resonance and anti-resonance is small; the effective electromechanical coupling factor is smaller, thus the transferred acoustic energy decreases. These pairs are in the curves 6 and 8 on Figures 5 and 6, respectively.

In fact, considering the window of frequencies, one can see that resonance and anti-resonance pair displacements depend on l_a. Each pair enters to the window by superior limit with low k_{eff}. As this pair becomes close to the reference resonance, k_{eff} increases. But again, near the inferior limit of the window, k_{eff} decreases. Figure 9 shows k_{eff} as function of l_a.

Resonances, anti-resonances and k_{eff} curves present gradual decreasing average as function of water column height. Load influence pushes f_r, f_a and k_{eff} downwards to the unloaded reference. Looking at the curves peaks in Figure 9, one can notice that the electromechanical coupling factor decreases with load height and, as consequence, each associated vibration mode becomes weaker. An increasing load mass implies on a k_{eff} tendency to decay [24]. In practice, decreasing of k_{eff} implies in diminishing the difference between f_a and f_r and their respective impedance moduli, Z_a and Z_r. Sometimes these differences become too small that is not easy to be detected experimentally. Besides, near the resonance, other modes of vibration often arise and the impedance *versus* frequency curve may present many resonance / anti-resonance pairs (and their corresponding electromechanical coupling factors) [26], making difficult the identification of the mode that

provides greater piezoelectric conversion. Therefore, a better conversion performance cannot be achieved considering only one resonance. The electronic circuitry should perform a search for the best resonance, by sweeping inside the frequency window required for system operation. The decision for a new working frequency should be based on the higher value of k_{eff}.

These findings were only possible because of our larger frequencies window span, which allowed the perception of new resonances / anti-resonance pairs, in contrast to the results obtained in [6].

The physical perception of the new resonance / anti-resonance pairs and their effective electromechanical coupling factors offers a better understanding on the behavior of the electrical impedance on the piezoelectric ring. The design of electronic driving circuits including new strategies of frequency control may derive from these findings.

5. CONCLUSIONS

Resonances, anti-resonances and effective electromechanical coupling factors of a piezoelectric ring, mechanically loaded with water, and vibrating in the thickness mode has been studied. The experimental and calculated results show: resonances / anti-resonances of the piezoelectric ceramic decrease as the load is increased, and new pairs of resonances / anti-resonances (and their corresponding electromechanical coupling factors) arise; the effective electromechanical coupling factor of each resonance changes, such as the higher k_{eff} are always near at reference resonance.

Electronic driving circuits used for the piezoceramics should thus run algorithms that consider the frequency sweep, and seek the higher k_{eff} in order to provide the best resonance.

6. ACKNOWLEDGMENT

Authors thank to FAPESP-SP-Brazil for the financial support of this work (Proc. 2012-07639-4).

References

[1] Y. Sasaki, M. Umeda, S. Takahashi, M. Yamamoto, A. Ochi, T. Inoue, "High-power characteristics of multilayer piezoelectric ceramic transducers," *Japanese J. Applied Physics*, vol. 40, no. 9B part 1, pp. 5743-5746, Sept. 2001.

[2] S. O. Ural, S. Tuncdemir, Y. Zhuang, K. Uchino, "Development of a high power piezoelectric characterization system and its application for resonance/antiresonance mode characterization," *Japanese J. Applied Physics*, vol. 48, no. 5R, May 2009.

[3] B. Dubus, G. Haw, C. Granger, O. Ledez, "Characterization of multilayered piezoelectric ceramics for high power transducers," *Ultrasonics*, vol. 40, no. 1-8, pp. 903-906, May 2002.

[4] F. J. Arnold, S. S. Mühlen, "The resonance frequencies on mechanically pre-stressed ultrasonic piezotransducers," *Ultrasonics*, vol. 39, no. 1, pp. 1-5, Jan. 2001.

[5] F. J. Arnold, S. S. Mühlen, "The mechanical prestressing in ultrasonic piezotransducers," *Ultrasonics*, vol. 39, no. 1, pp. 7-11, Jan. 2001.

[6] L. Shuyu, "Load characteristics of high power sandwich piezoelectric ultrasonic transducers," *Ultrasonics*, vol. 43, no. 5, pp. 365-373, Mar. 2005.

[7] K. Komatsu, "Constant vibration amplitude method of piezoelectric transducer using a PLL (Phase Locked Loop)," *Japanese J. Applied Physics*, vol. 24, no. S1 , pp. 159-162, Jan. 1985.

[8] B. Mortimer, T. du Bruyn, J. Davies, J. Tapson, "High power resonant tracking amplifier using admittance locking," *Ultrasonics*, vol. 39, no. 4, pp. 257-261, Jun. 2011.

[9] A. Ramos-Fernandez, F. Montoya-Vitini, J. A. Gallego-Juarez, "Automatic system for dynamic control of resonance in high power and high Q ultrasonic transducers," *Ultrasonics*, vol. 23, no. 4, pp. 151-156, Jul. 1985.

[10] S. C. Tang, G. T. Clement, "A harmonic cancellation technique for an ultrasound transducer excited by a switched-mode power converter," *IEEE Trans. Ultrasonics, Ferroelectrics Frequency Control*, vol. 55, no. 2, pp. 359-367, Feb. 2008.

[11] C. Ying, Z. Zhaoying, Z. Ganghua, "Effects of different tissue loads on high power ultrasonic surgery scalpel," *Ultrasound Medicine Biology*, vol. 32, no. 3, pp. 415-420, Mar. 2006.

[12] G. Kossoff, "The effects of backing and matching on the performance of piezoelectric ceramic transducers," *IEEE Trans. Sonics Ultrasonics*, vol. SU 13, no. 1, pp. 20-30, Mar. 1966.

[13] T. Noguchi, A. Fukumoto, "Diagnostic study of bonded, thickness mode transducers by input impedance measurement," *IEEE Trans. Sonics Ultrasonics*, vol. SU 20, no. 4, pp. 365-370, Oct. 1973.

[14] T. Inoue, M. Ohta, S. Takahashi, "Design of ultrasonic transducers with multiple acoustic matching layers for medical application," *IEEE Trans. Ultrasonics, Ferroelectrics Frequency Control*, vol. 34, no. 1, pp. 8-16, Jan. 1987.

[15] R. N. Thurston, "Effects of electrical and mechanical terminating resistances on loss and bandwidth according to the conventional equivalent circuit of a piezoelectric transducer," *IRE Trans. Ultrasonics Eng.*, vol. 7, no. 1, pp. 16-25, Feb. 1960.

[16] C. S. Desilets, J. D. Fraser, G. S. Kino, "The design of efficient broad-band piezoelectric transducers," *IEEE Trans. Sonics Ultrasonics*, vol. 25,

no. 3, pp. 115-125, May 1978.

[17] S. van Kervel, J. Thijssen, "A calculation scheme for the optimum design of ultrasonic transducers," *Ultrasonics*, vol. 21, no. 3, pp. 134-140, May 1983.

[18] J. H. Goll, B. Auld, "Multilayer impedance matching schemes for broadbanding of water loaded piezoelectric transducers and high Q electric resonators," *IEEE Trans. Sonics Ultrasonics*, vol. SU 22, no. 1, pp. 52-53, Jan. 1975.

[19] W.P. Mason, *Electromechanical Transducers and Wave Filters*, New York, USA, Van Nostrand Company, 1948.

[20] D. Berlincourt, D. Curran, H. Jaffe, "Piezoelectric and piezomagnetic materials and their function in transducers," *W.P. Mason, Physical Acoustics*, vol. I-A, ch. 3, 1964.

[21] R. Krimholtz, D. Leedom, G. Matthaaei, "New equivalent circuits for elementary piezoelectric transducers," *Electron. Lett.* , vol. 6, no. 13, pp. 389-399, Jun. 1970.

[22] A. Ballatto, "Modeling piezoelectric and piezomagnetic devices and structures via equivalent networks," *IEEE Trans. Ultrasonics, Ferroelectrics Frequency Control*, vol. 48, no. 5, pp. 1189-1240, Sept. 2001.

[23] G. Martin, "On the theory of segmented electromechanical systems," *J. Acoustical Soc. America*, vol. 36, no. 7, pp. 1366-1370, Jul. 1964.

[24] W. Toulis, "Electromechanical coupling and composite transducers," *J. Acoustical Soc. America*, vol. 35, no. 1, pp. 74-80, Jan. 1963.

[25] *IEEE Standard on Piezoelectricity*,ANSI/IEEE Std 176-1987, 1987.

[26] R. Silva, M. Franco, P. Neves Jr., H. Bartelt, A. Pohl, "Detailed analysis of the longitudinal acousto-optical resonances in a fiber Bragg modulator," *Optics Express*, vol. 21, no. 6, pp. 6997-7007, Mar. 2013.

Francisco J. Arnold received the physics graduation degree from University of São Paulo State (UNESP), Rio Claro, São Paulo, Brazil, in 1986; the M.Sc. degree in Applied Physics from University of São Paulo (USP), Ribeirão Preto, São Paulo, Brazil, in 1990; and the Ph.D. degree in Electric Engineering from University of Campinas (UNICAMP), Campinas, São Paulo, Brazil, in 1995. Since 1994, he is with School of Technology of UNICAMP, Limeira, São Paulo, Brazil. His research activities are in the areas of piezoelectric transducers and electronic instrumentation.

Marcos S. Gonçalves received the B.S. degree in electrical engineering from the National Institute of Telecommunication, Santa Rita do Sapucai, in 1998, Brazil, MS, and PHD in electrical engineering from the University of Campinas in 2002, and 2007, respectively, Brazil. From 2007 to 2009, he was with School of Electrical and Computer Engineering of the University of Campinas as a researcher. Since 2009, he has been a professor with the School of Technology of the University of Campinas. His research interests include computational physics, computer-aided engineering, and photonic and microwave devices.

Leonardo L. Bravo-Roger received the B. S. and M.Sc. degree in Telecommunication Systems from University of Oriente (UO), Santiago de Cuba, in 1985 and 1998, respectively, and the Ph.D. degree in Electric Engineering from Faculty of Electrical and Computer Engineering, University of Campinas (UNICAMP), Campinas, São Paulo, Brazil, in 2003. Since 2004, he is with School of Technology of UNICAMP, Limeira, São Paulo, Brazil. His research activities are in the areas of RF and microwave technologies and radar sensing systems and Wireless Sensor Networks.

Sérgio Muhlen received the B.Sc. and M.Sc degrees in electrical engineering from the University of Campinas (Unicamp), Brazil, in 1982 and 1985, respectively; and the D.Sc degree in biomedical engineering from the Institut National Polytechnique de Lorraine, France, in 1989. He worked at the McGill University in Montreal, Canada, during a sabbatical year (2007), and at the Ecole Centrale de Lyon, France, in a three-month stage (2010). He is currently Associate Professor at the Department of Biomedical Engineering / FEEC-Unicamp. His research interests include medical equipment, power ultrasound, clinical engineering and risk management and hospital resources, electromagnetic interference in health environment, and biological effects of electrical fields.